ELSEVIER

Evaluation of the calibration errors on cooling of a differential scanning calorimeter using different sets of standard metals

M.J.A. Malheiro [a], J.A. Martins [a,*], J.J.C. Cruz Pinto [b]

[a] *IPC, Departamento de Engenharia de Polímeros, Universidade do Minho, 4800-058 Guimarães, Portugal*
[b] *CICECO, Departamento de Química, Universidade de Aveiro, 3810-193 Aveiro, Portugal*

Abstract

The temperature calibration on cooling of thermal analysis instruments is important for the accurate study of the non-isothermal crystallization kinetics of semi-crystalline polymers. In previous works, a methodology was proposed for performing the calibration on cooling of differential scanning calorimeters (DSCs) with standard metals, and the calibration errors were checked using transitions of high-purity liquid crystals. In this work, alternative, physically meaningful, procedures for carrying out the calibration on cooling are analyzed and validated. The calibration errors are evaluated also with liquid crystalline transitions, when the calibration is performed with standard metals, in a wide temperature range, and when due account is taken for the need of isothermal corrections to the temperature measurements. It is shown that any pair of standard metals may be used to calibrate on cooling, that the calibration errors increase for wider working temperature ranges and that, providing that certain conditions are fulfilled, both calibration procedures yield similar results.
© 2004 Elsevier B.V. All rights reserved.

Keywords: DSC temperature calibration on cooling; True sample temperatures

1. Introduction

The first known work on methods for the calibration on cooling of thermal analysis instruments was that of Höhne et al. [1]. It was based on experiments performed with liquid crystals, where it was suggested that, for the same scanning rate, the heating and cooling thermal lags were symmetrical. As far as it is known, practical applications of this calibration procedure were not widely implemented, neither the calibration errors evaluated. Following the suggestion presented therein for implementing the calibration on heating, it is assumed that an average isothermal correction is evaluated for a large temperature range, the correction being the same for heating and cooling experiments. For a particular standard, the rate-dependent thermal lag, $\Delta T_{tot} = T_{true} - T_e(\beta)$, where T_e is the extrapolated onset fusion temperature, is evaluated for a particular heating rate, β, and the gradient $\Delta T_e/\Delta \beta$ calculated, from which the isothermal

correction may finally be determined. Average values of the above gradient were suggested for metals and organic substances. In that same work, the asymmetry of the heat transfer during heating and cooling modes, originated by an incorrect adjustment of the electronic system, is identified as a source of difficulty in performing the calibration on cooling of power compensation DSCs.

Another procedure for performing DSC [2] and differential thermal analyser [3] calibrations on cooling was proposed by Menczel and Leslie. This procedure makes use of liquid crystalline transitions of high-purity liquid crystals for calibrating those instruments. The calibration errors of this procedure were evaluated by means of a set of cooling experiments at different cooling rates, performed over the same liquid crystals.

A method previously proposed by two of the present authors for calibrating thermal analysis instruments on cooling from heating calibrations at the same scanning rate with standard metals also makes use of two basic assumptions: the symmetry of the scanning rate components of the thermal lags for heating and cooling experiments, and a constant (temperature-independent) isothermal deviation [4].

* Corresponding author. Tel.: +351 253510325; fax: +351 253510339.
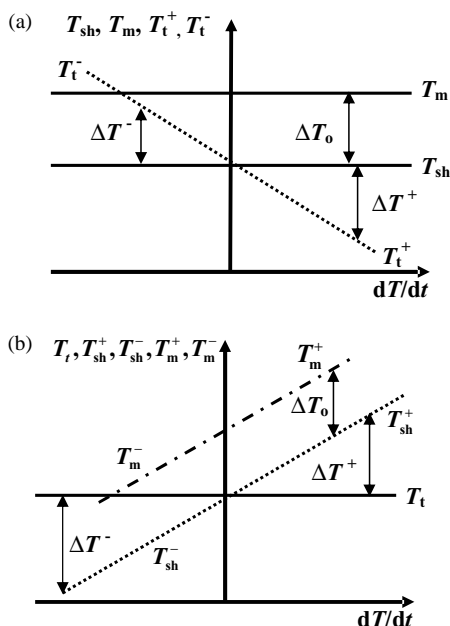 *E-mail address:* jamartins@dep.uminho.pt (J.A. Martins).

Fig. 1. Schematic representation of the procedures used for performing the calibration on cooling from the calibration on heating. (a) Method 1: a given but arbitrary measured temperature (or ideal sensor temperature) is assumed for a particular heating and cooling rate, the true sample temperature being lower for heating scans and higher for cooling scans. (b) Method 2: a given real sample temperature is assumed for a particular heating and cooling rate, the rate-dependent measured temperature (or ideal sensor temperature) being higher, for heating scans, and lower, for cooling scans, than the sample temperature.

The isothermal deviation (ΔT_0) may be positive, negative or zero and it may be set to the latter value (at least at a given temperature) by proper hardware adjustment. If the temperature measured by the sample holder temperature sensor, T_m, in isothermal conditions, equals the temperature that an ideal, properly calibrated, temperature sensor would read, T_{sh}, the isothermal deviation ($\Delta T_0 = T_m - T_{sh}$) is of course zero. An isothermal correction could instead have been defined as Höhne et al. [1], but the results obtained are not affected by these different definitions. Assuming that the instrument's measurement cell is fitted with such perfect sensors, a temperature calibration over samples with high thermal conductivity just requires accounting for the thermal lag originated by the scanning rate. For a particular heating rate, the true sample temperature is lower than that measured by the sample holder temperature sensor, while for a cooling rate of the same magnitude the opposite should occur. A graphical scheme is shown in Fig. 1a. If, at the same scanning rate and sensor temperature, those true sample temperatures are T_t^+ and T_t^-, for heating and cooling scans, respectively, the symmetry between the heating and cooling thermal lags may be expressed as

$$\Delta T^- = -\Delta T^+ \Leftrightarrow T_t^- - T_{sh} = -(T_t^+ - T_{sh}), \qquad (1)$$

and the calibration on cooling may be performed from the calibration on heating by

$$T_t^- = 2T_{sh} - T_t^+. \qquad (2)$$

This equation shows that, for the same scanning rate, the temperature measured by the sample holder temperature sensor is the average of the true sample temperatures for heating and cooling scans.

Since the measured temperature, T_m, is generally different from T_{sh} (cf. above), the true sample temperature on cooling, expressed as a function of T_m, is

$$T_t^- = (2 - a^+)T_m - b^- \qquad (3)$$

with $b^- = 2\Delta T_0 + b^+$, where ΔT_0 is the isothermal correction and a^+ and b^+ are evaluated from the calibration on heating for the same scanning rate ($T_t^+ = a^+ T_m + b^+$).

Another possible procedure for performing this calibration is by defining the thermal lag originated from the scanning rate with respect to each true sample temperature value, T_t, for any heating or cooling scan. Fig. 1b describes this second procedure.

For a particular scanning rate, the true sample temperature may now be defined as the average of the measured temperatures for that scanning rate, in heating and in cooling,

$$T_t = \tfrac{1}{2}(T_{sh}^- + T_{sh}^+) = \tfrac{1}{2}(T_m^- + T_m^+ - 2\Delta T_0), \qquad (4)$$

which may be written in a form similar to that of Eq. (1), expressing the symmetry of the thermal lags originated by the scanning rate,

$$\Delta T^- = -\Delta T^+ \Leftrightarrow T_t - T_{sh}^- = -(T_t - T_{sh}^+). \qquad (5)$$

Writing Eq. (4) with respect to the measured temperature during cooling experiments results in

$$T_t = \frac{a^+}{2a^+ - 1}T_m^- - \frac{b^+}{2a^+ - 1} - \frac{2a^+}{2a^+ - 1}\Delta T_0, \qquad (6)$$

which reduces to Eq. (3) when $a^+ = 1$. For a power compensation DSC, at ordinary scanning rates, this condition often holds to within better than 1% (and seldom worse than within 2%).

The true temperature evaluated from Eq. (3) or (6) is only representative of the real sample temperature for samples with negligible thermal resistance, such as samples of metal standards currently used for temperature calibrations. For other samples, the thermal resistance must be accounted for and, for evaluating the sample's temperature during a transition, the possible effect of the latent heat absorbed or released during the phase change must also be considered for [5,6].

2. Experimental

The experiments were performed in a Perkin Elmer DSC7, run in standard mode. The temperature of the cold block
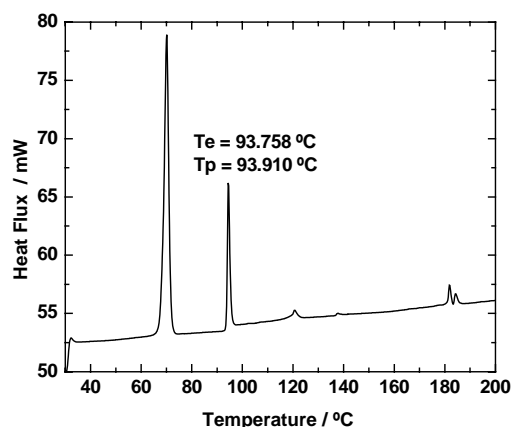
Fig. 2. DSC curves for the HP53 liquid crystal. Experiment performed with temperature and heat flow rate calibrations at 16 °C/min. Sample mass = 4.515 mg.
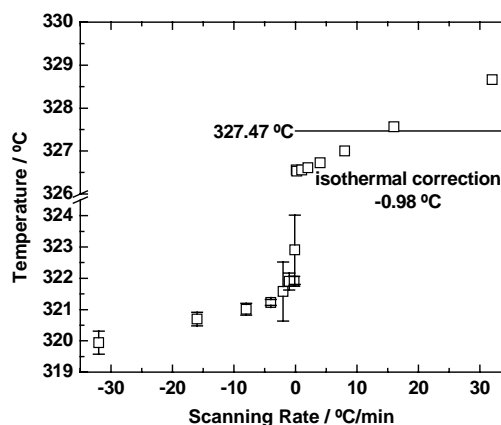

Fig. 3. Onset temperatures for the melting and crystallization of lead. Results recorded without the temperature calibration of the instrument. Sample weight = 4.569 mg. The cooling experiments were repeated five times and the error bars show the standard deviations of the mean.

was kept constant, at 5 °C, the purge gas flow rate was 20 cm³/min and 30 μl aluminum pans with holes were used for all experiments. The standard metals used in the temperature calibrations were indium, tin, lead and zinc, the first three from Goodfelow with purities of 99.99999, 99.9999 and 99.99%, respectively. The zinc standard was supplied by Perkin Elmer and has an unspecified purity.

The liquid crystal used, supplied by Merck, was 4-(4-pentyl-cyclohexyl)benzoic acid-4-propyl-phenyl ester, with the brand name of HP53. A DSC scan of this liquid crystal is shown in Fig. 2. The liquid crystalline transition used for checking the calibration on cooling was T_e = 93.758 °C (onset) and T_p = 93.910 °C (peak). Values of the transition temperature, assumed as the real values, were obtained by extrapolating the corrected heating onset results to zero scanning rate ($T_{e,t}$ = 93.738 °C).

3. Results and discussion

An important step for performing the temperature calibration on cooling is the evaluation of the isothermal correction and its temperature dependence in the temperature range of work. Fig. 3 shows the procedure used for this evaluation at the lead melting temperature. The value found was −0.98 °C. The figure also shows the average values obtained for cooling scans, after a set of five experiments performed over the same sample, and the results clearly reveal the existence of a non-negligible supercooling during crystallization. The error bars show the standard errors of the mean. The basic assumption that led to the establishment of Eqs. (3) and (6), for performing the calibration on cooling from the calibration on heating with standard metals, was the symmetry of the rate-dependent components of the thermal lags. The results of Fig. 3, obtained before the actual temperature calibration, do not make clear that symmetry, mainly because of the isothermal correction at 327.47 °C and the supercooling of lead, estimated previously as 2.17 °C

[4]. For other standard metals, e.g. tin, showing larger supercoolings, this symmetry is even less evident [7], and this may have contributed to some standard metals not being recommended for temperature calibrations on cooling [8]. It will be shown in this work that, providing that the isothermal correction (including its temperature dependence), and the rate-dependent thermal lags are properly evaluated, any combination of standard metals may be used for that purpose.

The magnitude of the isothermal correction and of its temperature dependence do change during the instrument's working life and, for accurate measurements, they should be evaluated with some regularity, preferably before and after a set of measurements. The magnitude of this correction, for the instrument used in this work, and for temperatures ranging from the indium to the zinc melting temperatures, is shown in Fig. 4. This correction may be assumed to be roughly linear for temperatures ranging from 156.6 °C up to 327.47 °C, while for higher working temperatures its non-linearity must be taken into account for accurate temper-
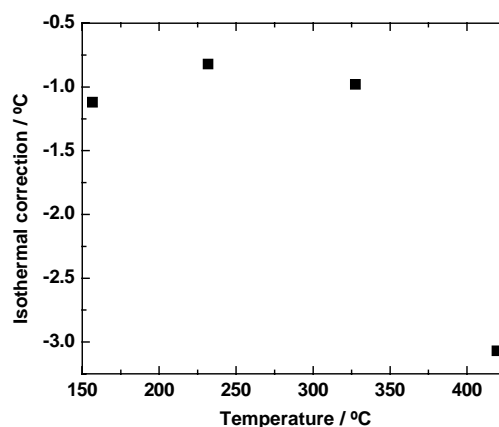

Fig. 4. Isothermal correction at the melting temperatures of indium, tin, lead and zinc.
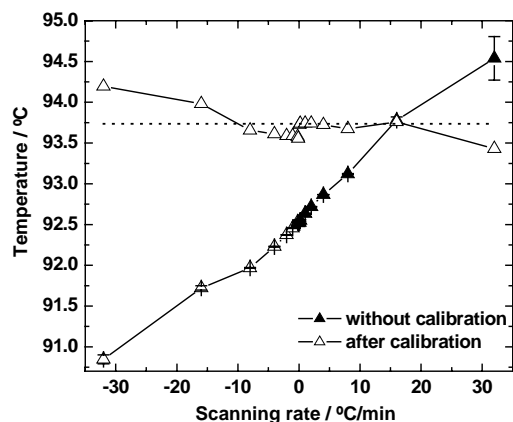
Fig. 5. Onset temperatures for the liquid crystalline transition of the HP53 liquid crystal. The full symbols (▲) are the results before calibration and the open symbols (△) are the results after the calibration on heating (performed with two standards) and on cooling, according to Eq. (3), method 1. Each heating and cooling experiment was repeated three times and the error bars show the standard deviations of the mean; sample weight = 4.515 mg.

Table 1
Calibration errors for the calibration on cooling performed according to Eqs. (3) and (6)

dT/dt (°C/min)	Onset temperature (°C)	
	Method 1, Eq. (3)	Method 2, Eq. (6)
−32	−0.437	−0.439
−16	−0.223	−0.224
−8	0.101	0.100
−4	0.147	0.147
−2	0.169	0.169
−1	0.170	0.170
−0.2	0.179	0.180
−0.1	0.203	0.204

The errors presented were measured with respect to the temperature obtained by extrapolating the corrected onset values for the heating experiments of Fig. 5 to zero scanning rate.

ature calibrations. Since we could not find high-purity liquid crystals for checking the temperature calibration on cooling at high temperatures, the isothermal correction at the indium melting temperature and its linear temperature dependence, evaluated from the indium, tin and lead data of Fig. 4, will be used in this work. The purpose is the comparison of the errors obtained by using one or the other procedure.

The application of the heating and cooling temperature calibration procedures, the last one with Eq. (3), method 1, to the liquid crystalline transition of HP53 of Fig. 2, is illustrated in Fig. 5. From the data in the figure it is clear that this liquid crystalline transition shows a supercooling of 0.2 °C (certainly small, but possibly not entirely negligible, e.g. for accurate calibration purposes). For the heating experiments, the deviation from the expected result (93.738 °C, dashed line) only becomes noticeable for scanning rates of 32 °C/min and higher. For cooling rates up to −1 °C/min, the changes in the predicted temperatures are very small indeed, but they increase for higher cooling rates, in a direction opposite to the expected one, considering the expected increase of the degree of supercooling with the cooling rate.

The temperature calibration for the results of Fig. 5 was performed following method 1, Eq. (3). This calibration may also be performed with method 2, Eq. (6). The errors of these two calibration procedures are in Table 1 and include the transition's supercooling at zero cooling rate and the eventual (unknown) temperature dependence of transition supercooling with the cooling rate, together with the "true" temperature calibration errors. For these two calibration procedures, the temperature dependence of the isothermal correction was neglected, the assumed isothermal correction being that measured at the indium melting temperature. The comparison of the results obtained with the two methods show very small differences that are mainly the result of the

calibration constant a^+ being close to 1, around 0.98 in this case. For these situations, the two calibration procedures are expected to yield similar results.

Additional points worth discussing are the temperature calibration in a broad temperature range and the use of different sets of standard metals for performing the calibration on cooling, together with the errors associated to the calibration procedures. These are shown in Figs. 6 and 7.

In Fig. 6 the results of Fig. 5 are compared with those obtained when the temperature calibration is performed with the four metal standards by finding, for each particular heating rate, the constants a^+ and b^+ that best describe a linear relation between the expected and measured temperatures for the four standards. The calibration on cooling was performed from the calibration on heating with Eq. (6). An increase of the calibration errors is of course expected when the calibration is performed for a wider temperature range. Considering the expected result shown by the dashed line
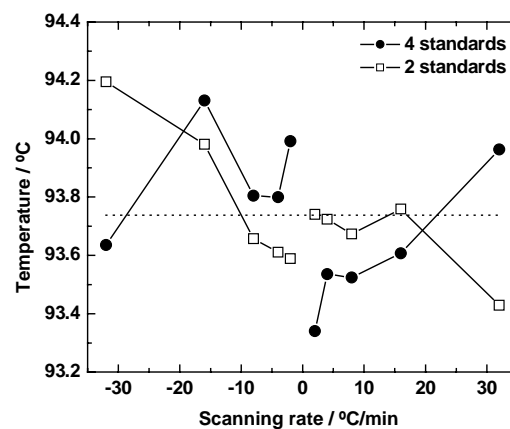

Fig. 6. Differences between the temperature calibration on heating and cooling when it is performed with two and four metal standards. The dashed line is the expected temperature for ideal heating and cooling calibrations. The open squares (□) are the onset results for the temperature calibration performed with two metal standards, as in Fig. 5, and the full circles (●) are for the temperature calibration performed with four metal standards.
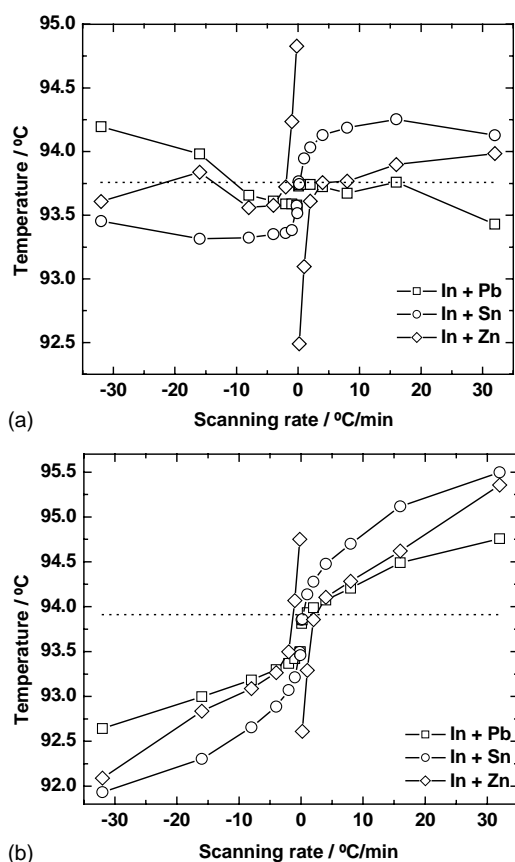
(a)

(b)

Fig. 7. Predicted temperatures for the liquid crystalline transition of HP53 with the temperature calibration on heating and cooling for different pairs of standard metals. (a) Onset and (b) peak temperatures of the transition. The dashed line in (a) represents the expected temperature obtained by extrapolating the corrected onset valued to zero scanning rate (93.738 °C), while the dashed line in (b) represents the result obtained following the same procedure as in (a) but for the peak temperature value (93.91 °C).

in the figure, the results obtained indicate that the calibration on cooling may be performed from the calibration on heating in a wide temperature range, with errors of ±0.4 °C for cooling rates from −2 °C/min up to −32 °C/min. An increase of the temperature calibration errors is also expected for increasing cooling rates. The results for lower cooling rates, from −0.1 to −1 °C/min are not shown in the figure because of the difficulty in getting results within acceptable experimental error limits for the melting of zinc at those scanning rates. Nevertheless, these results are collected in Fig. 7.

In Fig. 7a, the results of Fig. 5 are compared with those obtained when the temperature calibration is performed with two other pairs of metal standards. The largest deviation is observed for the pair indium–zinc at the lowest cooling rates. The results shown in this figure indicate that the calibration on cooling may be performed from the calibration on heating, using any pair of standard metals, with an error of ±0.5 °C for cooling rates up to −32 °C/min. As previously mentioned, the zinc results for cooling rates from −0.1 to −1 °C/min are not included in the analysis. While in Fig. 7a

Table 2
Temperature calibration errors for the calibration on cooling with method 2, but accounting for the temperature dependence of the isothermal correction

dT/dt (°C/min)	Onset temperature (°C)	
	ΔT_0(In)	ΔT_0(linear variation)
−32	−0.439	−0.537
−16	−0.224	−0.324
−8	0.100	−0.001
−4	0.147	0.044
−2	0.169	0.066
−1	0.170	0.068
−0.2	0.180	0.076
−0.1	0.203	0.100

the results shown refer to the onset temperature of the liquid crystal transition, Fig. 7b shows the results obtained for the peak temperature of the same transition. The deviations shown in the latter figure are much higher, indicating that the nature of the transition is of first order, as confirmed by the DSC scan of Fig. 2.

The above results were obtained assuming a constant value of the isothermal correction at the indium melting temperature. If, now, a linear variation of the isothermal correction with temperature is assumed, the corresponding results are those shown and compared with the previous ones in Table 2. For all of these results, method 2 was used for correcting the temperatures on cooling. The variation implied by this temperature-dependent isothermal correction on the results obtained is of just 0.1 °C, which is within the instrument's experimental measurement errors and may, in a first instance, be neglected.

4. Complementary discussion

The temperature corrections presented previously are only applicable to samples with low thermal resistance, such as metal standards, where even for thick samples the thermal gradients along their thickness are small. The errors for the calibration on cooling increase with the cooling rate, as expected, and we may assume an error limit of ±0.5 °C in the temperature calibration for cooling rates up to −32 °C/min. Although this may seem a large value for a power compensation DSC instrument, accounting for this error in non-isothermal crystallization experiments over polymer samples is important for accurate analysis, such as in the evaluation of the average true sample temperature at a particular cooling rate and the use of this information for predicting the average spherulite size [5–7].

The temperature of a polymer sample is also dependent on the sample mass and the temperature profiles along the sample thickness may be important for evaluating the average true sample temperature. A quantitative evaluation of the temperature profile and the average sample temperature requires accounting for the different heat transfer phenomena

within the sample in the DSC oven, and also accounting for the latent heat absorbed or released during any non-athermal phase change. Previous simulations of the temperature profile of relatively thick DSC samples (around 1 mm) have shown that it may be assumed to be parabolic, with the sample's bottom and top at the same temperature, the program temperature [7]. Thick samples may be considered to be heated by conduction from the sample's bottom and top, and the effective thickness to be considered for evaluating the average true sample temperature is half the overall thickness. For thinner samples, the gas layer trapped inside the pan is responsible for a different temperature at the top of the sample (lower than the bottom for heating scans and higher for cooling scans), and the entire sample thickness, with the adequate conductive and/or convective boundary conditions, should then be considered for evaluating the sample's temperature profile.

Samples of polyethylene were prepared with controlled dimensions, with the purpose of evaluating, as accurately as possible, the sample's thermal resistance. Two polyethylenes were selected, one a GPC standard material with $\bar{M}_w = 32\,100$ g/mol, $\bar{M}_w/\bar{M}_n = 1.1$ at 139.59 °C. The other was a commercial linear low-density polyethylene (LLDPE) with MFI = 0.55 g for 10 min, evaluated according to the ISO 1133 standard, a density of 926 kg/m^3 at 139.8 °C. The mass, thickness and area of the samples were 7.532 mg, 0.227 mm and 6.86 mm^2 for the GPC standard PE and 22.603 mg, 0.95 mm and 6.86 mm^2 for the commercial LLDPE, respectively. For the thermal conductivity of the materials, the value considered was 0.42 W/(K m).

Both samples were melted above their thermodynamic melting temperature, the temperature being kept stable for a period longer than 5 min, and the sample was then cooled with a controlled cooling rate of −10 °C/min. The purpose was to induce a controlled morphology at the start of all experiments. After cooling to room temperature, the sample was again melted at controlled heating rates ranging from 2 to 32 °C/min. Heating scans were used for these analyses since, in principle, the temperature calibration on heating may be performed with greater accuracy. The results obtained for the two materials show that neither the peak nor the onset melting temperatures were coincident for the different heating rates used, which indicate that, even after the implementation of appropriate calibration procedures, the true sample temperature is different from the recorded program temperature. An example of the results obtained for the commercial LLDPE sample is shown in Fig. 8a.

The true sample temperature may be estimated for heating scans by subtracting from the measured temperature the product of the sample's thermal resistance by the heat flux corrected relative to the baseline, which only assumes quasi-steady-state heat transfer conditions. A more accurate estimate requires solving a first order differential equation describing the transient heat transfer within the sample while it absorbs its heat of fusion [5,6]. The results obtained are shown in Fig. 8b for the commercial LLDPE sample, and
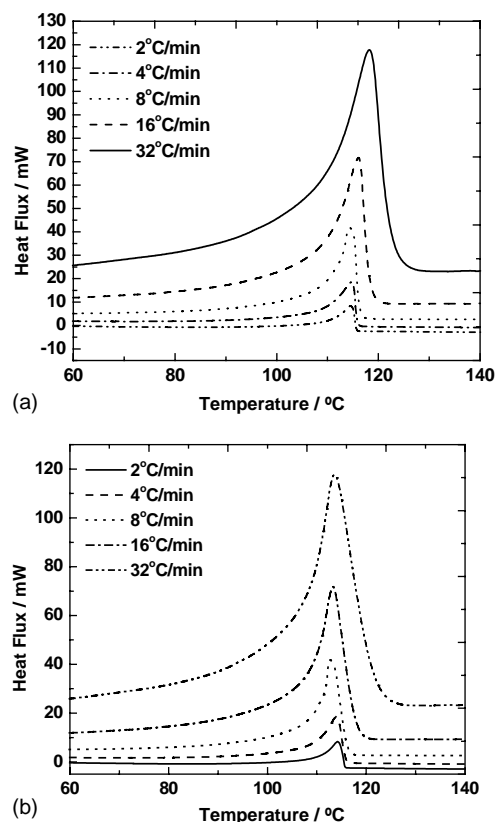

(a)

(b)

Fig. 8. Melting of a commercial grade of a linear low-density polyethylene at the heating rates indicated after a controlled cooling at −10 °C/min. (a) Results obtained after the calibration on heating at the rates indicated; (b) results obtained after the evaluation of the true sample temperatures, by accounting for the sample's thermal resistance and latent heat absorbed during the phase change; sample mass = 22.603 mg.

in Fig. 9 for the GPC standard PE. They show that, for the GPC standard, the average sample temperature is given by the onset of the peak, while for the commercial material it is given by the peak value of the corrected curves, and they
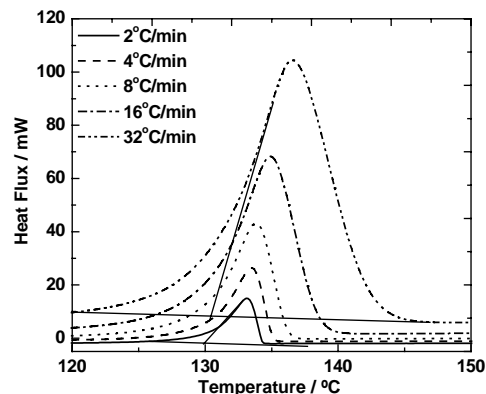

Fig. 9. Melting of a PE GPC standard at the heating rates indicated, after a controlled cooling at −10 °C/min. The results shown were obtained after the true sample temperature evaluation, by accounting for the sample's thermal resistance and the latent heat absorbed during the phase change; sample mass = 7.532 mg.
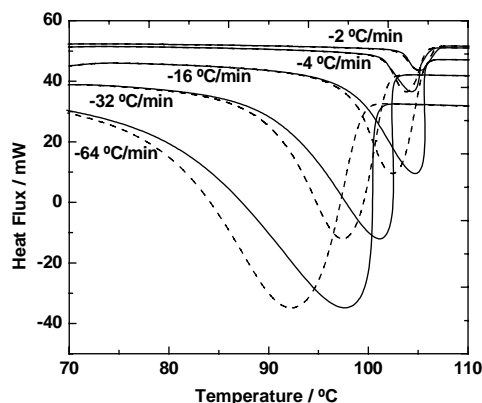
Fig. 10. Non-isothermal crystallization experiments for the linear low-density polyethylene sample of Fig. 8, at the rates indicated. The dashed lines are the results for the calibration on cooling, including the temperature dependence of the isothermal correction. The full lines are for the results obtained after the true sample temperature evaluation, which include the joint effects of the sample thermal resistance and the latent heat absorbed during the phase change.

are both slightly lower than the corresponding values for the uncorrected curves, the difference significantly increasing with the heating rate, as physically expected.

An example of the results of implementing these corrections to cooling experiments is shown in Fig. 10, for the crystallization of the commercial LLDPE sample at different cooling rates. The dashed lines show the results obtained after the implementation of the calibration on cooling, while the solid lines refer to the corrected average sample temperatures. The differences between the two curves become increasingly important for higher cooling rates. The results of Figs. 8b, 9 and 10 clearly show the importance of evaluating the average true sample temperatures, in addition to the implementation of appropriate sensor temperature calibration procedures.

5. Conclusions

1. Two alternative temperature calibration methods for cooling scans in differential scanning calorimeters have been developed and validated. They are simply based on a transform of the calibration for heating scans.
2. Providing that both an isothermal and a scanning rate-dependent sensor temperature correction are performed, accurate temperature calibrations to within $\pm 0.4\,^{\circ}C$ in a wide temperature range may be achieved, for cooling scans from -2 to $-32\,^{\circ}C/min$.
3. Contrary to some previous suggestions, any pair of standard metals may be used in temperature calibrations on cooling.
4. Accurate sample temperature evaluations, however, require accounting for the additional effects of the sample's thermal resistance and possible heat release/absorption during the thermal scan on the unsteady-state heat flow balance within the sample.

References

[1] G.W.H. Höhne, W. Heminger, H.-J. Flammersheim, Differential Scanning Calorimetry, An Introduction for Practitioners, Springer-Verlag, Berlin, 1996.
[2] J.D. Menczel, T.M. Leslie, J. Therm. Anal. 40 (1993) 957.
[3] J.D. Menczel, J. Therm. Anal. 49 (1997) 193.
[4] J.A. Martins, J.J.C. Cruz Pinto, Thermochim. Acta 332 (1999) 179.
[5] J.A. Martins, J.J.C. Cruz Pinto, True sample temperature in isothermal DSC scans and their effect on the overall crystallization kinetics, J. Appl. Polym. Sci. 91 (2004) 125.
[6] J.A. Martins, M.C. Cramez, M.J. Oliveira, R.J. Crawford, J. Macromol. Sci. Phys. B 42 (2003) 367.
[7] J.A. Martins, M.A. Malheiro, J.C. Teixeira, J.J.C. Cruz Pinto, Thermochim. Acta 391 (2002) 97.
[8] S.M. Sarge, G.W.H. Höhne, H.K. Cammenga, W. Eysel, E. Gmelin, Temperature, heat and heat flow rate calibration of differential scanning calorimeters in the cooling mode, in: Proceedings of the 12th ICTAC, Copenhagen, 2000, p. 152.